IMPROVEMENT OF A HYDROSTATIC TRANSMISSION CONTROL SYSTEM PERFORMENCE USING RADIAL BASIS NEURAL NETWORK

Dr. Amjad Jalil Humadi
(Lecturer)
University of Technology
Control and Systems Engineering Department

Ayad Qasim Hussein
(Assist. Lecturer)
Foundation of Technical Education
Electrical and Electronics Technical College

Mashael Matti Farjo
(Assist. Lecturer)
Foundation of Technical Education
Electrical and Electronics Technical College

ABSTRACT

Pump-controlled motors (PCM) are the preferred power elements in most applications because of their high maximum operating efficiency. The dynamics of such hydraulic systems are highly nonlinear and the system may be subjected to non-smooth and discontinuous nonlinearities. Aside from the nonlinear nature of hydraulic dynamics, hydraulic servo systems also have large extent of model uncertainties such as uncompensated friction forces variation of system parameters and external disturbances. The conventional Proportional, Integral and Derivative (PID) controller can not cope with hydraulic system nonlinearities and could not compensate its variation of parameters. Therefore, a radial basis neural network has been suggested to control the speed response of PCM. The structure of radial basis neural network (RBNN) controller is simple and efficient in control purposes. The design of control surface based on radial basis function (RBF) controller has been considered. The performance of PID and RBF controllers has been assessed based on the improvement in speed behavior and their capabilities to compensate the changes in system parameters (load and bulk of modulus). Also, the effect of tuning of the radial basis parameters on the dynamic response has been studied. Results showed that the RBF controller is more robust and shows typical results compared to classical PID controller. Moreover, a further improvement in speed dynamic can be obtained with appropriate tuning of RBF parameters.

KEYWORDS: Hydrostatic transmission, PID controller, radial basis neural network controller.

الخلاصة:

تستخدم المحركات المسيطر عليها باستخدام الضاغط الهايدروليكي (pump-controlled hydraulic motors) في تطبيقات كثيرة وذلك لكفائة اشتغالها العالية. تمتلك مثل هذه المنظومات خواص لاخطية عالية وكذلك تتعرض خلال الاشتغال الى تغيرات لاخطية ومتقطعة (discontinuous nonlinearities). لغرض السيطرة على سرعة المنظومة الهايدروليكية فان المسيطر التقليدي (التناسبي ، التفاضلي ، التكاملي) يفشل في توليد اشارة سيطرة تلم او تعوض (compensate) عن الطبيعة اللاخطية المنظومة وهذا يتطلب استخدام مسيطر غير تقليدي (ذكي) لمعالجة مثل هذه المشاكل. حيث تم في هذا البحث استخدام مسيطرعصبي شبكي (neural network) وتم تصميم سطح السيطرة (control surface) الذي يشكله هذا المسيطر. علاوة على ذلك تمت دراسة تأثير متغيرات المسيطر الذكي (intelligent controller) على أداء استجابة السرعة للمنظومة الهايدروليكية. حيث تبين من النتائج الممثلة باستخدام الحاسبة بأن أداء المنظومة بوجود المسيطر العصبي الشبكي يتفوق على أدائها بوجود المسيطر المناظر (التقليدي) وكذلك تبين من النتائج بان المسيطر العصبي الشبكي له قابلية عالية في كبت تاثيرالتغيرات المفاجئة وتأثير التغير في معلمات المنظومة على أداء السرعة للمنظومة الهايدروليكية.

1. INTRODUCTION

Pump controlled motor are the preferred power element in applications which required considerable horsepower for control purpose because of their high maximum operating efficiency which can approach 90% in practice. However, the comparatively slow responses of these elements limit their use in high performance systems [Merrit 1967, Watton 1989].

Variable displacement piston pump is usually accomplished with a swash plate that has a variable degree of angle. As the piston barrel assembly rotates, the pistons rotate around the shaft, with the piston shoes in contact with and sliding along the swash plate surface. Since there is no reciprocating motion when the swash plate is in vertical position, no displacement occurs. As there is an increase in the swash plate angle, the pistons move in and out of the barrel as they follow the angle of the swash plate surface. The pistons move out of the cylinder barrel during one half of the cycle of rotation thereby generating an increasing volume, while during the other half of the rotating cycle, the pistons move into the cylinder barrel generating a decreasing volume. This reciprocating motion results in the drawing in and pumping out of the fluid. Pump capacity can easily be controlled by altering the swash plate angle, larger the angle, greater being the pump capacity. A cross-sectional view of this pump is shown in Fig.(1) [Ravi 2005, Noah 2001].

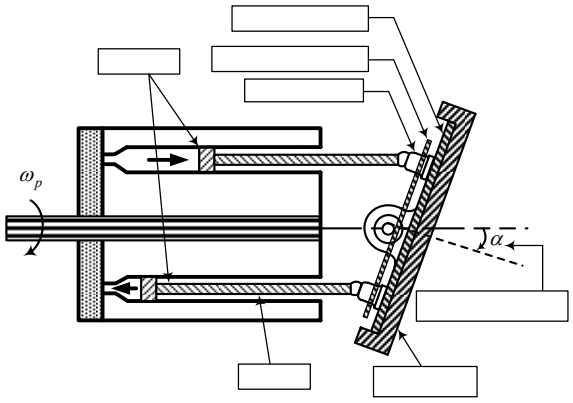

Figure (1) *Variable-displacement pump*

The basic pump-controlled motor, often called a hydrostatic or hydraulic transmission, is shown schematically in Fig. (2). A variable displacement pump, driven by a constant speed power source and capable of reversing the direction of the flow, is directly connected to a fixed displacement hydraulic motor. Hence, the motor speed and direction of rotation may be controlled by varying the pump stroke [Merrit 1967, Ali 2006].

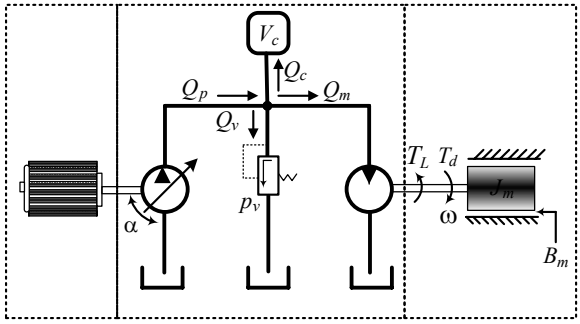

Figure (2) *Pump-controlled Motor*

A replenishing supply is required to replace leakage losses from each line and to establish a minimum pressure in each line. This auxiliary supply is a constant pressure type with low capacity because only leakage flows are supplied. The replenishing supply prevents cavitations and air entrainment because it pressurize each line and helps dissipate heat by providing cooler fluid to replace the leakage [Merrit 1967].

Safety relief valves are used in the lines to protect system from damage due to pressure peaks. These valves establish an upper limit to the line pressure and are set to operate above normal operating pressures. Theses valves must respond rapidly and have a large capacity because they must pass the maximum pump flow in an extreme overload. These valves should be connected across the lines so that overload flow is dumped to the other line to help prevent cavitations [Merrit 1967, Ali 2006].

2. MATHEMATICAL MODEL

It is assumed that the angular velocity of the prime mover (induction motor) and hence the angular velocity of the pump shaft ω_p is constant. Pump flow rate can be varied by adjusting the swashplate displacement angle and the flow-angle relationship can be given as [Ravi 2005, Ali 2006].

$$Q_p = (K_p \eta_{vp})\, \alpha \qquad (1)$$

where, Q_p is pump flow rate (m^3/s), α is displacement angle of swashplate (◦), K_P is pump coefficient (m^3/s), η_{vp} is pump volumetric efficiency which is assumed not to depend on pump rotation angle.

To simplify the analysis, pressure relief valve dynamics is not taken into consideration. Therefore, two equations are given for passing

flow rate through pressure relief valve (m^3/s) in state of opening and closing as follows:

$$Q_v = \begin{cases} K_v\,(P - P_v) & P > P_v \\ 0 & else \end{cases} \quad (2)$$

or,

$$Q_v = \lambda\, K_v\,(P - P_v) \quad (3)$$

where, K_v is slope coefficient of valve static characteristic $(m^5/N.s)$, P is system pressure (P_a), P_v is valve opening pressure (P_a) and λ is given by:

$$\lambda = \begin{cases} 1 & P > P_v \\ 0 & P \le P_v \end{cases} \quad (4)$$

If, it is assumed that pressure drop in the hydraulic hose is negligible:

$$Q_c = (V/\beta)(dP/dt) \quad (5)$$

$$(dP/dt) = (\beta/V)Q_c \quad (6)$$

where, Q_c is flow rate deal with fluid compressibility (m^3/s), V is the fluid volume (m^3) subjected to pressure effect, β is fixed bulk modulus (P_a). Flow rate used in the hydraulic motor can be written as in [Ravi 2005, Ali 2006];

$$Q_m = K_m\,\omega_m / \eta_{vm} \quad (7)$$

where, K_m is hydraulic motor coefficient (m^3), ω_m is angular velocity of hydraulic motor (rad/s) and η_{vm} is volumetric efficiency of the motor. Hydraulic motor torque (N.m) can be written as:

$$T_d = (K_{mt}\,\eta_{mm})\;P \quad (8)$$

where T_d is the developed torque (N.m), K_{mt} is motor torque coefficient (m^3), P is the pressure drop in hydraulic motor (P_a) and η_{mm} is mechanical efficiency of hydraulic the motor. The developed torque T_d produced in the hydraulic motor is equal to the sum of the moments from the motor loads and can be given as, [Merrit 1967]

$$T_d = J_m\,\dot{\omega}_m + B_m\,\omega_m + T_L \quad (9)$$

where, J_m is the inertia of the hydraulic motor shaft $(N.m.s^2)$, B_m is viscous friction coefficient of motor and its shaft $(N.s/m)$. From Fig.(2), one can deduce

$$Q_p = Q_c + Q_m + Q_v \quad (10)$$

From Eqs.(1-7), one can write Eq.(10) as

$$\dot{P} = -\lambda\left(\frac{\beta K_v}{V}\right)P - \left(\frac{\beta K_m}{V\eta_{vm}}\right)\omega_m + \left(\frac{\beta K_p\,\eta_{vp}}{V}\right)\alpha + \lambda\left(\frac{\beta K_v}{V}\right)P_v \quad (11)$$

Similarly, from Eqs.(8-9), the following equation will result

$$\dot{\omega}_m = \left(\frac{K_m\,\eta_{mm}}{J_m}\right)P - \left(\frac{B_m}{J_m}\right)\omega_m - \left(\frac{1}{J_m}\right)T_L \quad (12)$$

Setting x_1, x_2 and u as P, ω and α, respectively, the following state-space form can be obtained

$$\left.\begin{aligned} \dot{x}_1 &= \lambda\; a_{11}\; x_1 + a_{12}\,x_2 + b_{11}u + \lambda.b_{12}\,P_v \\ \dot{x}_2 &= a_{21}\; x_1 + a_{22}\,x_2 + b_{21}\;T_L \end{aligned}\right\} \quad (13)$$

where

$a_{11} = -(\beta.K_v)/V$, $a_{12} = -(K_m\;\beta)/(V\;\eta_{vm})$,

$a_{21} = (K_{mt}\,\eta_{mm})/J_m$, $a_{22} = -B_m/J_m$

$b_{11} = (\beta\;K_p\,\eta_{vp})/V$, $b_{12} = (\beta\;K_v)/V$,

$$\lambda = \begin{cases} 1 & x_1 > P_v \\ 0 & x_1 \le P_v \end{cases}$$

One can argue that Eq.(13) acquire its nonlinearity from the nonlinear coefficient λ and the saturation of control signal u, where it should not exceed maximum angular displacement; i.e., $u_{\max} = \alpha_{\max}$, which is equal to 16^o in the present application.

3. RADIAL BASIS STRUCTURE

A radial basis function neural network is shown in Fig.(2). There, the inputs are x_i, $i = 1,2,\ldots,n$ and the output is $y = F_{rbf}(x)$ where $F_{rbf}(x)$ represents the processing by the entire radial basis function neural network. Let $x = [x_1, x_2, \ldots, x_n]^T$. The input to the i^{th} receptive field unit (sometimes called a radial basis function) is x, and its output is denoted with $R_i(x)$. The receptive field unit has what is called a "strength" which is

denoted by b_i . Assume that there are n_R receptive field units. Hence, from Fig.(3), [Dan 2001,Yu 2002]

$$y = \sum_{k=1}^{nR} b_k \, R_k(x) \qquad (14)$$

is the output of the radial basis function neural network. If Gaussian radial basis is chosen, then

$$R_k(x) = \exp\left(\frac{(x - c^k)^2}{(\sigma^k)^2} \right) \qquad (15)$$

where $c^k = [c_1^k, c_2^k, \ldots, c_n^k]$, σ^k is a scalar.

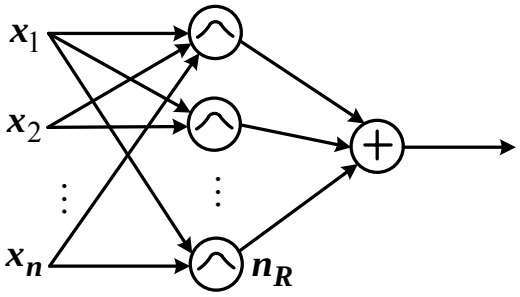

Figure (3) *Radial basis function neural network model*

For the case where $n=1$, $c^1=[c_1^1]=2$ and $\sigma^1 = 0.1$, $R_1(x)$ is shown in Fig.(4) [Kevin 2006],

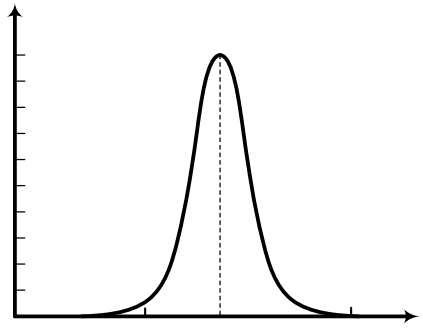

Figure (4) *Radial neuron activation*

4. TRADITIONAL TUNNING OF PID CONTROLLER

In order to use a controller, it must first be tuned to the system. This tuning synchronizes the controller with the controlled variable, thus allowing the process to be kept at its desired operating condition. Standard methods for tuning controllers and criteria for judging the loop tuning have been used for many years. Some of them are mathematical criteria, Ziegler-Nichols Cohen-coon method, trial and error method, continuous cycling method, relay feed-back method and Kappa-Tau tuning method. From the above mentioned methods, Ziegler-Nichols method is the most common one and will be adopted here in the present work as a traditional method of tuning PID parameters [Astrom 1995, Michael 2005].

The design based on this method is based on knowledge of the point on the Nyquist curve of the process transfer function where the Nyquist curve intersects the negative real axis. For historical reasons this point is characterized by the parameters K_u and T_u, which are called the *ultimate gain* and the *ultimate period* Fig.(5).

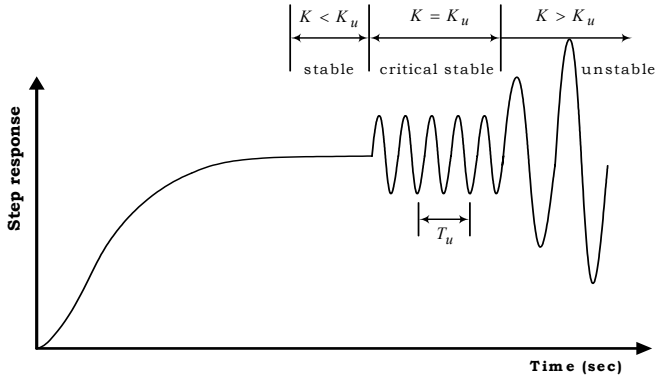

Figure (5)*: Characterization of a step response in the Ziegler-Nichols frequency response method.*

The formulas, given by Ziegler-Nichols, which relating the parameters of the PID controller, and the ultimate gain and ultimate period are listed in Table (1). It should be noted that Table (1) applies for the design of P (proportional) and PI controllers in addition to the PID controller with the same set of experimental data from the plant.

Table (1): *PID controller parameters obtained from the Ziegler- Nichols frequency response method.*

Controller	k_p	k_I	k_d
P	$0.5K_u$	---	---
PI	$0.4K_u$	$0.8T_u$	---
PID	$0.5K_u$	$0.5T_u$	$0.125T_u$

5. DESIGN AND SYNTHESIS OF RBF CONTROL SURFACE [Kevin 2006]

Figure (6) shows the speed control of hydrostatic transmission system based on RBF controller. The

inputs to the radial basis function neural network will be the error and change of error, respectively,

$$e = \omega_r - \omega \quad (16)$$

$$\dot{e} = \dot{\omega}_r - \dot{\omega} \quad (17)$$

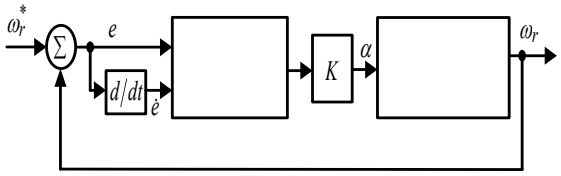

***Figure (6)**: Hydrostatic transmission system.*

Lets consider a radial basis function neural network with $n=2$ inputs, and $n_R = 11$ so we will have to pick 11 strength b_i, $i=1, 2...11$. Based on simulations of step response of the PCM speed, the maximum excursions (dimensions) of the error and change of error can be estimated as

$$e(k) \in [-3e^5, 3e^5] \quad (18)$$

$$c(k) \in [-6e^5, 6e^5] \quad (19)$$

For the respective field units we use spread σ_j^i (i.e. so that the size of the spread depends on which input dimension is used) with

$$\sigma_j^i = 0.7\frac{espan}{\sqrt{n_R}}, \sigma_j^i = 0.7\frac{cespan}{\sqrt{n_R}} \quad (i=1,2...11) \quad (20)$$

where *espan* and *cespan* are the maximum excursions of error and change of error, respectively. It is worthy to note that they, *espan* and *cespan*, can be estimated via simulation. For σ_j^i, the ($espan/11$) factor makes the spread size depend on the number of grid points along the e input dimension (similarly for σ_j^i), and the 0.7 factor was chosen to get a smooth interpolation between adjacent respective field units.

To design radial basis function neural network for the angular velocity problem, we simply need to choose the b_i, i=1, 2…11, parameters to shape the mapping in the approximate way. Suppose that we view parameter as being loaded in a matrix,

$$\begin{bmatrix} b_1 & b_{12} & b_{23} & b_{34} & b_{45} & b_{56} & b_{67} & b_{78} & b_{89} & b_{100} & b_{111} \\ b_2 & b_{13} & b_{24} & b_{35} & b_{46} & b_{57} & b_{68} & b_{79} & b_{90} & b_{101} & b_{112} \\ \vdots & \vdots & \vdots & \vdots & \vdots & \vdots & \vdots & \vdots & \vdots & \vdots & \vdots \\ b_{11} & b_{22} & b_{33} & b_{44} & b_{55} & b_{66} & b_{77} & b_{88} & b_{99} & b_{110} & b_{121} \end{bmatrix}$$

***Figure (7)**: Control Surface of RBNN Controller*

The entries of matrix B is based on the controller action.

One can note that if $e=c=0$, the actual speed is not deviating from the reference speed hence, the controller sets the control signal u=0; i.e., the angular position of α is set to zero and no change of speed appears. In this case, the value of $b_{61} = 0$.

If; however, the error e is near positive maximum value and that c is positive and near a maximum positive value, then the angular speed of hydraulic motor is moving to become even worse than it currently is. In this situation, the neural network controller will produce the largest positive control signal $u_{\max}$ to actuate the pump plate such as to counteract the effects of having a change of velocity in the wrong direction. Then the value of b_{121} is set to $u_{\max}$.

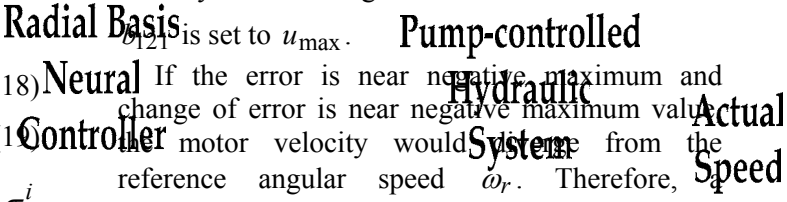

If the error is near negative maximum and change of error is near negative maximum value, the motor velocity would diverge from the reference angular speed ω_r. Therefore, a maximum negative actuating signal is necessary to be fed to the pump plate such that the pump would give the required pressure to pull down the velocity to reference speed in a minimum time. Consequently, the value of b_1 is given value of $-u_{\max}$.

As the error reaches maximum positive value and change of error reaches maximum negative value, then the actual speed approaches the reference with high rate. This situation is also repeated if the error reaches maximum negative value and the change of error reaches maximum positive value, the motor velocity runs quickly to reference value. At such cases, no actuating signal is fed to the pump plate, as no need to give any pressure signal to hydraulic motor. Therefore, the values of b_{11} and b_{111} are set to zero. Based on the above argument, the stimulus-response characteristic of the RBNN, we have just designed, can be depicted in the form of a control surface and is illustrated in Fig.(7). One can note that the plot summarizes the (decisions) that the neural network will make.

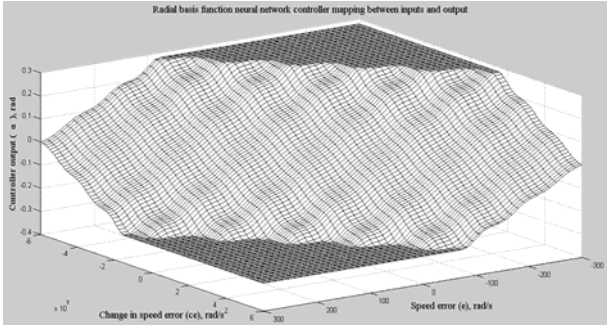

***Figure (8)** Speed responses of the PID controller*

6. RESULTS

For simulation purposes, we have used a backward difference approximation to the derivative, i.e.,

$$\dot{e} = \frac{e(kT) - e(kT - T)}{T}$$

where T is the sampling period and k is an index for the time step (k). The step size in this work is chosen to be 5×10^{-5} and the system differential equations have been solved using fourth order Runge-Kutta. The program code used for implementing the neural network controller, solving governing differential equations of the hydrostatic transmission system (pump and hydraulic motor) and simulating different system behaviors has been written in MATLAB/m-file. The simulation time has been selected to be 0.04 seconds for most simulated results.

For setting the parameters of PID controller using Zeigler-Nichols method, one should connect the controller to the process such that the control action is proportional only, i.e., $Ki = 0$ and $Kd = 0$. The proportional gain is increased slowly until the process starts to oscillate as shown in Fig.(8). The gain when this occurs is K_u and the period of the oscillation is T_u. It is found that the value of K_u which makes the response oscillatory is equal to 2×10^{-3}. From the oscillatory response the value of T_u is equal to 0.04. Based on Table (1), one can by now determine the values of PID controller parameters:

$Kp = 1\times10^{-3}$, $Ki = 9\times10^{-4}$, $Kd = 2.25\times10^{-4}$

Setting these values into their corresponding parameters, the PID controller based response would be set up.

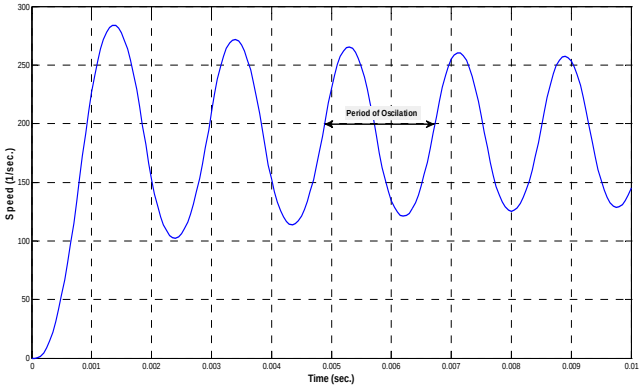

Figure (9) shows the speed dynamic behaviors based on both controllers. The comparison of the two controllers is evaluated in terms of transient parameters such as peak overshoot, rise time and steady-state error. It is evident from Fig.(8) that the response due to RBF-based controller has an excellent dynamic; as no overshoot or oscillation is observed and the speed track the reference faster than that with PID controller case. However, the steady state value of the speed response based on RBF controller does not coincide with the reference value, but can be further reduced if sigma value, number of receptive field units and scaling gain has been increased. On the other hand, PID controller could overcome this problem by virtue of integration action; as the integrator continues integrating until zero steady-state value has been reached.

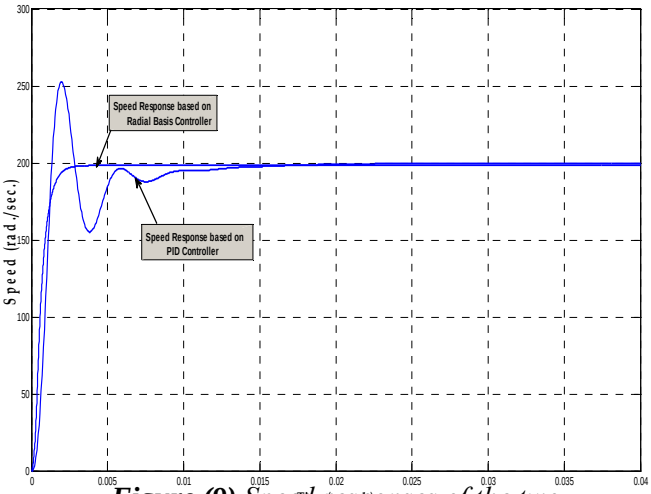

Figure (9) *Speed responses of the two controllers*

Upon the simulation run, the control signal would travel over the control surface like that shown in Fig.(10). This control surface has been synthesized based on all possible simulated (outcome) values of error and change of error. The equilibrium point where $\dot{e} = 0$ and $e = 0$ has been indicated in the figure.

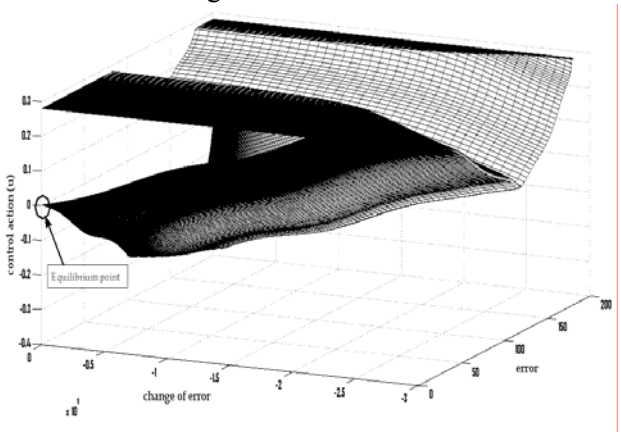

Figure (10) *Instantaneous input-otput mapping of RBF controllers*

In Fig. (11) the effect of changing the spread values (σ) of all Gaussian functions on the speed response is considered. The spread values are set at σ=0.3, 0.5 and 0.7. In this simulation, the number of receptive field units, over the ranges of error and its change, has been held to 121 units. One can see from the figure that setting spread value at 0.3 would show a limit cycle characteristics. With this small spread value, the Gaussian functions, responsible for synthesizing the control surface, would have high projections at their centers. This would produce a high steep hill and valleys surface, which in turn would make the solution at equilibrium point ($\dot{e} = e = 0$) to oscillated between these minima and maxima. Setting the spread values of the Gaussian functions at $\sigma = 0.7$ would better flattening the control surface and this would result in a smooth control surface near the equilibrium point. Therefore, the speed response is much improved. The decrease of steady-state error value due to increasing of spread values is attributed to the increase of control surface average value. This would boost the control signal to higher level and then decreasing the steady-state error.

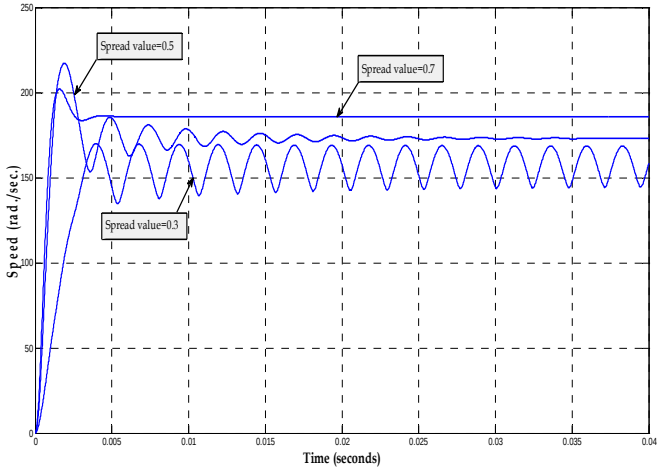

Figure (11) *Speed response with different spread values*

In Fig. (12-a), the number of receptive field units is changed. Three cases with 3, 5 and 6 number of units are considered. One can see clearly from the figure that the case with 3 numbers of units shows oscillatory characteristics, while the case with 9 numbers shows the best transient performance among the others. One can argue that the low number of receptive units would produce high ripple control surface, while high number of receptive units results in a smooth and monotonic control surface especially at the equilibrium points. Moreover, it is clear from the figure that increasing the number of such units would decrease the steady state error. This is a true deduction, since the slant of the control surface would be high with high number of receptive field units, and then the boosting of control signal near the equilibrium points would be so high.

Further increasing of receptive units would not affect considerably on the envelope of the control surface and, therefore, there is a small change in the transient response. However, the steady-state error continues decreasing with the increase of such unit numbers. This is such since the slope or gradient of the control signal near equilibrium points would further increase (see Fig.(12-b)).

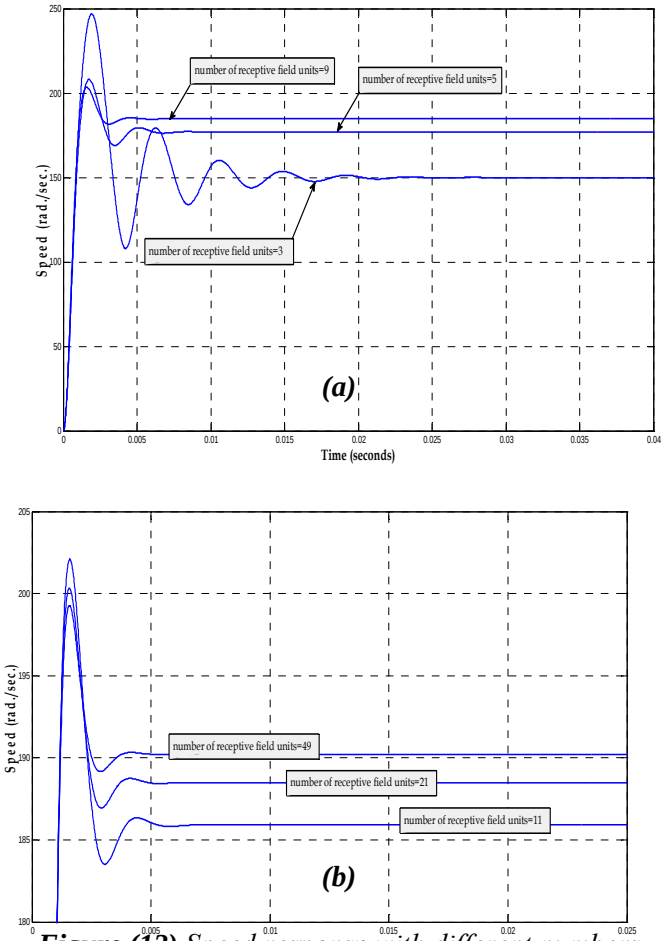

Figure (12) *Speed response with different numbers of receptive field unit values*

In Fig. (13), the scaling gain at the output of RBF has been varied at 0.5, 1 and 30. In this simulation, the number of receptive units is set at 11 and the spread value is fixed at a value of 0.7. The scaling gain has a large effect on the slope and envelope of the control surface. Low values of scaling gain would gives a small slant of the surface and this make the control signal to

swinging around the equilibrium points; i.e., an oscillation would arise. High value of scaling gain would make the control signal reaching the steady state in a fast fashion.

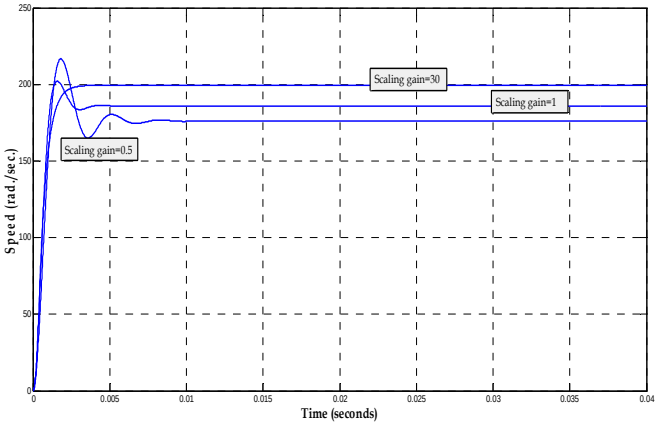

Figure (13) *Speed response with different scale gains*

In Fig.(14), a step load of $T_L = 25\ kN$ is exerted to the pneumatic system at time 0.03 second (to permit the transient response to come into settling condition). A comparison can be made between the speed responses based on these controllers. The height of change, due to load application, in speed response based on RBF controller is much lower than that with PID controller. Also, the speed behavior at time of load exertion shows an oscillatory characteristic before returning its steady state value, while the speed response with RBF shows a monotonic behavior and it reaches its previous value in a much lower time than its counterpart. The load rejection capability of RBF controller can be attributed to a large boost control signal to the swash-plate and then a high quantity of fluid would flow into the hydraulic motor with a low time. It is seen from the figure that the pressure latches at a specific negative value after a short time of load exertion; this is the required pressure to counteract the applied load.

In Fig.(15), the robustness of both controllers is again examined in terms of changing one of the system parameter (bulk of modulus of hydraulic fluid). Three responses has been simulated for each controller; one for fixed bulk of modulus (β), the other with 0.05% increment change in bulk of modulus ($\beta = \beta + 0.05\% \beta$) and the last plot is for 0.05% decrement change in bulk of modulus ($\beta = \beta - 0.05\% \beta$). The figure shows that there is degradation in speed response with PID controller when the value of bulk modulus has been decreased and an improvement when this value has been lowered. On the contrary, the change in speed response with RBF controller is much less than that with PID controller. Therefore, one can conclude that RBF-based controller is more robust than its counterpart.

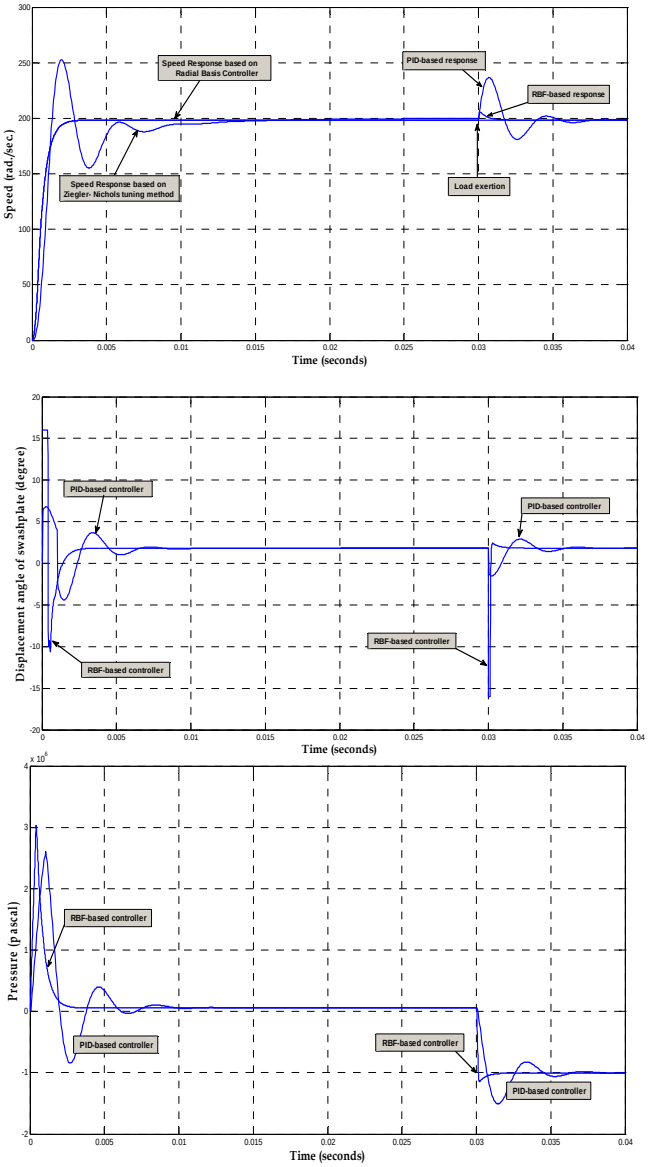

Figure (14) *Load rejection capabilities of both controllers*

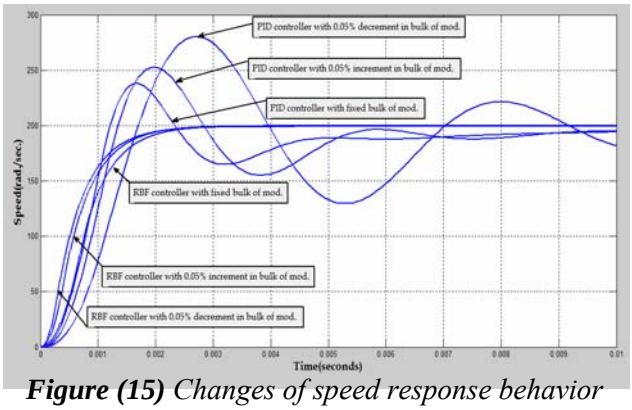

Figure (15) *Changes of speed response behavior of both controllers with change in bulk of modulus parameter.*

7. CONCLUSIONS

1. One can deduce from the simulated results that increasing the number of receptive field units could improve the control surface, and hence would enhance the dynamic performance of the speed response and lead to less steady state error. However, increasing the number of receptive units will increase the computation effect of executing the software program.
2. Increasing the scaling gain value could make the control surface steeper and then could bring the solution to steady state condition in a faster way with a minimum steady state error.
3. Increasing the spread value of the Gaussian function would make the controller surface flatter (i.e. become more even with fewer ripples). The solution, then, would slide on a smooth surface and no oscillation or peak-overshoot would appear.
4. If the hydraulic system is exerted to load changes or if it encounters change variation of parameters, the neural-base controller shows high load rejection capabilities and more robust characteristics than its counterpart.

REFERENCE:

Ali, V. A., "Effect of bulk modulus on performance of a hydrostatic transmission control system," Sadhana Vol. 31, pp. 543–556,Part 5, October 2006.

Astrom, K. J., Tore, H., "PID Controllers: Theory, Design and Tuning" Instrument Society of America, 1995.

Dan, J. S., "Training radial basis neural networks with the extended Kalman filter," Elsevier, 2001.

Kahaner, D., Moler, C., and Nash, S., "Numerical Methods and Software," Prentice-Hall, New Jersey, 1989.

Kevin, M. P., "Biomimicry for Optimization, Control, and Automation," Springer, 2005.

Merrit, H. E., "Hydraulic control systems," John Wiley & Sons, New York, 1967.

Michael, A. J., Mohamed, H. M.,"PID Control: New Identification and Design Methods," Springer-Verlag , 2005.

Noah D. Manring, Fikreadam A. Damtew "The Control Torque on the Swash Plate of an Axial-Piston Pump Utilizing Piston-Bore Springs", Journal of Dynamic Systems, Measurement and Control, 2001, Vol. 123.

Ravi Doddannavar, Andries Barnard, "Practical Hydraulic Systems," Elsevier Science & Technology Books, 2005.

Shampine, L. F., "Numerical Solution of Ordinary Differential Equations," Chapman & Hall, New York, 1994.

Watton, J., "Fluid power systems: Modeling, simulation, analog and microcomputer control," Englewood Chiffs, Prentice-Hall, 1989.

Yu, H.H., Jenq, N.H., "Hand book of Network signal processing," CRC Press, 2002.

APPENDIX

Table (2): *Parameters and coefficients*

Coefficient	Values
a_{11}	-2.1068e+003
a_{12}	-4.4120e+006
a_{21}	0.0945
a_{22}	-375
b_{11}	2.7465e+010
b_{12}	2.5281e+010
b_{22}	-3750
T_L	150
P_v	12e+6